Regional Trends in Weather Systems Help Explain Antarctic Sea Ice Trends

Journal Article

Author(s):
Schemm, Sebastian [iD]
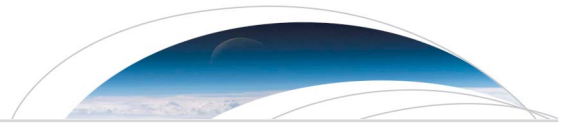
Key Points:
- Antarctic sea ice extent is strongly connected to regional cyclone and blocking frequencies
- Trends in Antarctic sea ice extent are often accompanied by significant trends in cyclone or blocking frequencies
- In some regions, spring sea ice extent is linked to autumn cyclones and blocks; in others, autumn sea ice extent is linked to spring blocks

Regional Trends in Weather Systems Help Explain Antarctic Sea Ice Trends

Sebastian Schemm[1] [ID]

[1]Institute of Biogeochemistry and Pollutant Dynamics and Institute for Atmospheric and Climate Science, ETH Zürich, Zürich, Switzerland

Abstract In contrast to Arctic sea ice extent, Antarctic sea ice extent has increased since 1979. On a regional scale, however, the trends exhibit high spatial variability and are even of the opposite sign. This study examines connections between sea ice extent and the frequencies of extratropical cyclones and blocks. Consideration is given to regions that exhibit long-term sea ice trends during spring and autumn. Significant connections exist in almost all examined regions. Typically, the region of maximum correlation is shifted upstream or downstream of the sea ice target region, which indicates that the 10-m wind associated with the examined weather systems is the chief thermodynamic and dynamic agent underlying sea ice variability. Along the ice edge of the Weddell and Ross Seas, the correlation between springtime sea ice extent and cyclone frequencies displays a wave number 3 pattern. Eastward of the Ross Sea, along the transition into the Amundsen Sea, spring sea ice extent is connected to cyclone and blocking frequencies during spring and the preceding autumn. Westward of the Ross Sea, autumn sea ice extent is strongly connected to blocking frequencies during the preceding spring. For the Bellingshausen Sea, an inverse relationship exists between autumn cyclone frequencies and autumn sea ice extent. Significant cyclone and blocking trends that are consistent with long-term sea ice trends exist in most examined regions. These findings point toward identifying regional trends in extratropical cyclone and blocking frequencies as a useful step toward a better understanding of couplings between Southern Hemisphere climate and regional trends in sea ice extent.

Plain Language Summary While most ice sheets and glaciers on Earth retreat, Antarctic sea ice extent has increased. But this increase is the residual of many regional trends of opposite sign. Current research activities focus on understanding why Antarctic sea ice trends exhibit so much spatial variability. This study shows that in most regions that exhibit strong trends in sea ice extent, a concomitant trend in the number of days affected by either a low-pressure system or a stationary, high-pressure system (atmospheric block) exists, which is in agreement with the trends seen in sea ice extent. Because it is known that the 10-m wind associated with these weather systems is an important driver of sea ice variability, these trends in weather systems help understand sea ice variability.

1. Introduction

During the past three decades (1979–present), Antarctic sea ice extent has increased (Comiso et al., 2017; Hobbs et al., 2016), a trend that is not well reproduced in climate models (Turner et al., 2013). On a regional level, the trends exhibit subtle differences or are even of opposite signs (Comiso et al., 2017; Hobbs et al., 2016; Parkinson & Cavalieri, 2012; Stammerjohn & Smith, 1997; Turner et al., 2016). Potential driving mechanisms underlying this trend asymmetry include changes in surface temperature (Comiso et al., 2017), wind direction (Hobbs et al., 2016; Holland & Kwok, 2012; Massom et al., 2008; Mayewski et al., 2009; Stammerjohn et al., 2003; Turner et al., 2016), sea ice drift (Pope et al., 2016), precipitation (Liu & Curry, 2010), ice-ocean feedbacks (Goosse & Zunz, 2014), and changes in the entrainment of warm deep water into the winter mixed layer (Zhang, 2007). A more comprehensive review of these and other mechanisms is provided by Hobbs et al. (2016). Past studies have focused on exploring connections between these inhomogeneous Antarctic sea ice trends and various climate modes (Hobbs et al., 2016; Kwok et al., 2016; Lefebvre et al., 2004; Pezza et al., 2012; Stammerjohn et al., 2003, 2008), and on the role of seasonal feedbacks (Holland et al., 2017; Holland, 2014).

Pinpointing the origin of regional sea ice extent anomalies is complex because anomalies can result from accumulated sea ice intensification rates during preceding seasons (Holland, 2014). For example, Holland (2014)

notes that in some regions, springtime intensification rates drive sea ice area anomalies during the following autumn. Furthermore, Holland et al. (2017) find that western Ross Sea sea ice extent in autumn is inversely connected to the 10-m zonal wind speed anomalies during the preceding spring. A natural question arising from this finding is whether this 10-m zonal wind speed anomaly is connected to any kind of anomalous weather system activity, for example, a persistent upstream block. A comprehensive study of the linkages between sea ice extent and the frequency of cyclones and blocks is therefore useful for understanding the linkages between trends in hemisphere-wide climate variability, regional sea ice extent, and the 10-m wind.

The aim of this study is to explore linkages between sea ice extent, cyclone and blocking frequencies, and long-term trends in both. The origin of many regional-scale sea ice trends is unclear, though trends in the 10-m wind are the chief candidate (Hobbs et al., 2016; Turner et al., 2016). On the hemispheric-scale, it is widely accepted that the Southern Annular Mode (SAM), a periodic equator-to-pole shift of the circumpolar-veering westerly jet stream, is affected by a long-term trend toward more poleward contracted westerlies (Marshall, 2003; Thompson & Solomon, 2002). The synoptic-scale circulation is an intermediate scale and connects the hemisphere-wide modes of Southern Hemisphere climate with the 10-m wind circulation. Consequently, this study attempts to (a) establish links between sea ice extent and the frequencies of cyclones and blocks, (b) quantify trends in the frequencies of both types of weather systems, and (c) examine whether such trends are in agreement with sea ice trends. This study focuses on spring and autumn because previous studies have suggested that autumn sea ice anomalies may originate from springtime wind anomalies (Holland et al., 2017; Holland, 2014).

The study is organized as follows: Data and methods are discussed in section 2. Section 3 discusses the relationship between sea ice fraction and the frequencies of cyclones and blocking. Section 4 examines trends in cyclones, blocks, and Antarctic sea ice.

2. Data and Methods

2.1. Data Availability

All atmospheric data used in this study are based on 6-hourly ERA-Interim data interpolated to a 1° × 1° regular grid. ERA-Interim data are publicly available via ECMWF's web interface: http://apps.ecmwf.int/datasets/. The sea ice data used in this study is the NOAA/NSIDC Climate Data Record of Passive Microwave Sea Ice Concentration, Version 3.1 (Meier et al., 2017; Peng et al., 2013), which is publicly available via the National Snow and Ice Data Center (NSICS) website: https://doi.org/10.7265/N59P2ZTG.

2.2. Cyclone and Block Detection

Cyclones are automatically detected by identifying and tracking, which are encompassed by a closed isobar (Wernli & Schwierz, 2006). Cyclone tracks are retained if they exist for longer than 24 hr. For an overview of the algorithm's performance relative to other existing methods, the reader is referred to the IMILAST intercomparison study (Neu et al., 2013). In general, there is a fairly good agreement between various cyclone detection schemes regarding the existence and location of deep systems; however, they differ more strongly for weak and short-lived depressions. It is therefore not surprising that the exact number of cyclones differs between various tracking methods and that trend estimates are method dependent (Grieger et al., 2018; Neu et al., 2013). In their comparison of 14 tracking methods during summer and winter around Antarctica, Grieger et al. (2018) find that most schemes agree on the sign of the trend, but the significance of the trend differs substantially between the methods.

Block detection relies on vertically averaged (between 500 and 150 hPa) negative anomalies in potential vorticity that persist locally for at least five consecutive days. Anomalies are defined as deviations from the climatological mean (Croci-Maspoli et al., 2007; Schwierz et al., 2006). The blocking and cyclone detections are based on 6-hourly ERA-Interim data interpolated to a 1° × 1° regular grid. The monthly mean cyclone and blocking frequencies used here are publicly available via an ETH Zürich-based web server: http://eraiclim.ethz.ch/ (Sprenger et al., 2017)

2.3. Trend Testing and Sensitivity of Point Correlations

To ensure field significance for the linear trends found in cyclone and blocking frequencies, the false discovery rate (FDR) was controlled using the procedure outlined in Wilks (2016). The FDR approach can be adopted whenever simultaneous multiple hypothesis tests need interpretation, as is this case when evaluating gridded data, which in this study are the t statistics of the linear trends. The threshold (α) that controls the multiple
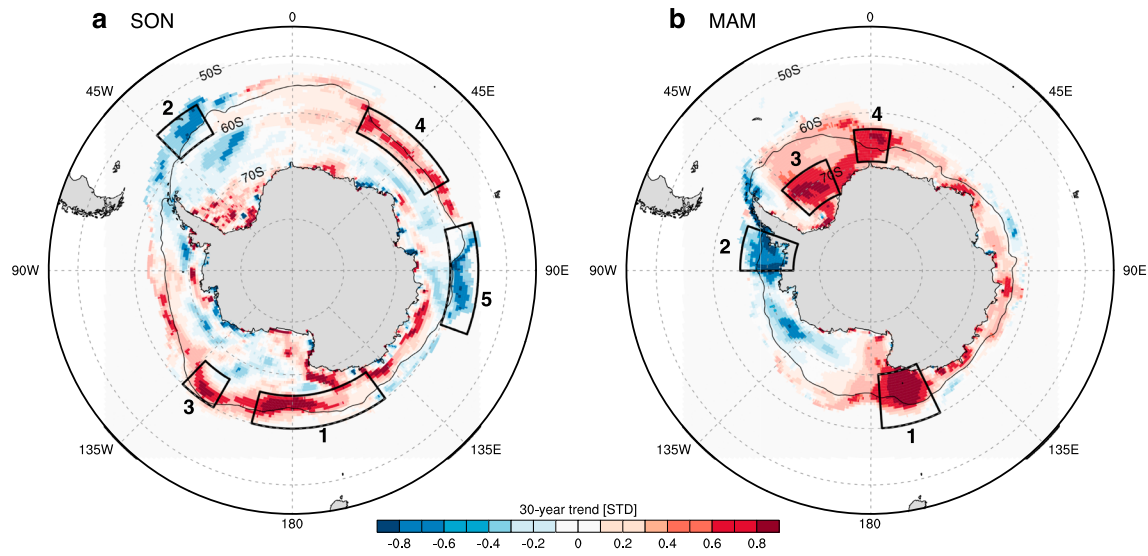
Figure 1. Standardized seasonal trends in sea ice fraction for (a) MAM and (b) SON. The black boxes indicate the target regions used for connecting sea ice trends with the frequencies of cyclones and blocks. MAM = Autumn (March-April-May); SON = Spring (September-October-November).

t statistics was set at 0.1. The FDR procedure yields a global $p*$, which is indicated by the stippling in Figure 5. This is a much stricter criterion than a stippling of all grid points with local p values smaller than 0.1.

For the point-correlations between cyclones, blocks, and area-averaged sea ice fraction, the significance is estimated from a t statistic. The correlations are typically only weakly sensitive to small shifts ($\pm 1° - 2°$) of the target boxes shown in Figure 1. The correlations are highest near the ice edge and lower near the continent.

3. Links Between Antarctic Sea Ice Trends and Trends in Weather Systems

What connects extratropical cyclone and blocking frequencies with sea ice extent anomalies is the 10-m wind and its role as a mechanical and thermodynamic agent (Comiso et al., 2017; Holland & Kwok, 2012; Lefebvre & Goosse, 2005; Massom et al., 2008; Mayewski et al., 2009; Turner et al., 2016). It would therefore be not surprising if many of the key areas, which exhibit strong trends in sea ice extent, are also affected by concurrent trends in weather systems. The target regions of interest are shown in Figure 1. Modest linkages where found between cyclone frequencies and sea ice extent during spring for the two target regions over the Indian Ocean sector (labeled 4 and 5 in Figure 1a); these regions are presented in the supporting information. During autumn, the weakest linkages, relative to the other target regions, are found for target regions 3 (which is not located along the ice edge where the linkages are typically largest) and 4 (Figure 1b), which are therefore presented in the supporting information.

3.1. Spring (September-October-November)

Over the first target region off the Ross Sea (black box labeled 1 in Figure 1), end-of-season sea ice extent is significantly correlated with seasonal cyclone frequencies (Figure 2a). At the same time, it is inversely correlated with blocking frequencies (Figure 2b). The maximum correlations are shifted slightly downstream of the target box such that the 10-m wind, veering cyclonically around a low-pressure system, advects consistently cold continental air over the sea ice (and vice versa for a high-pressure system). The correlation patterns for both types of weather systems display a zonal wave number 3 pattern. The centers of action are located downstream of South America, in the Indian Ocean sector between 45° – 90°E, and next to the target region. These three centers are fairly well confined along similar latitudes (55° – 65°S) but differ slightly in their longitude between the two types of weather systems. The sign of the correlation pattern changes farther poleward ($\sim$70°S), particularly for the cyclone frequencies.

Sea ice extent over the second target region (labeled 2 in Figure 1a), located off the Weddell Sea, also exhibits strong correlations with cyclone frequencies (Figure 2c). The maximum correlations are shifted slightly downstream relative to the target region. This downstream shift underpins the prominent role of the 10-m wind and the associated offshore advection of cold air and sea ice as relevant processes underlying sea ice
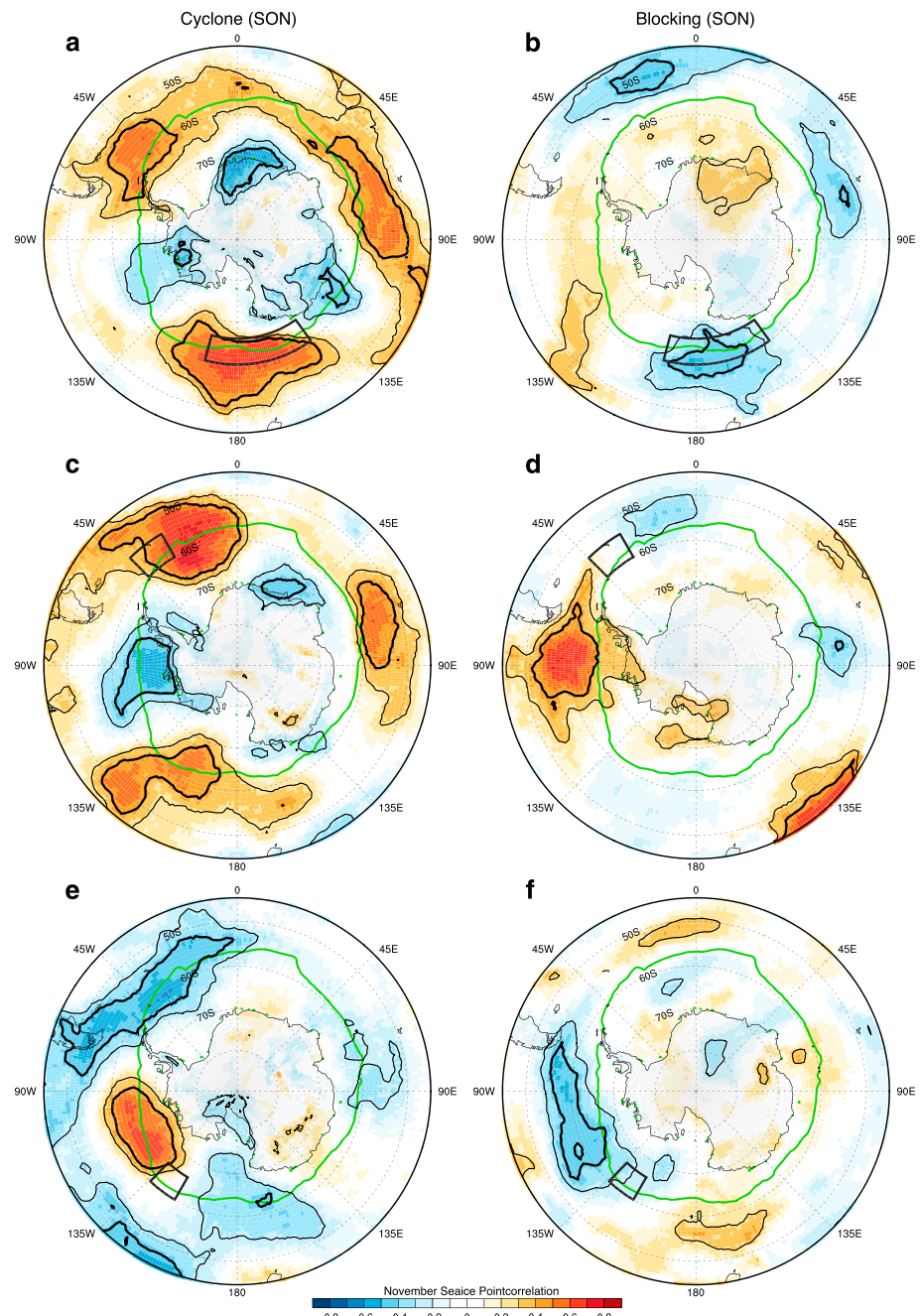
Figure 2. Point-correlation maps between November sea ice fraction, area-averaged over the different target regions (shown as black boxes in every panel), and SON cyclone (left column) and blocking (right column) frequencies. The thin black contour indicates statistical significance at the 0.9 level; the bold black contour indicates significance at the 0.99 level. The green contour indicates the climatological mean sea ice edge (15% sea ice fraction). SON = Spring (September-October-November).

variability in this region (Figure 2c). In agreement with the results from the first target region, the correlation between sea ice and cyclone frequency displays a zonal wave number 3 pattern, but the centers of action are in different locations (cf. Figures 2a and 2c). In contrast to cyclone frequencies, the correlation between sea ice and blocking frequency correlations display no zonal wave number 3 pattern (Figure 2d). Instead, a strong correlation center is found upstream over the Bellingshausen-Amundsen Sea and a second center at 135°E, indicating a wave number 2 pattern. In any case, anticyclonic winds veering around the center of a blocking system located over the Bellinghausen Sea direct offshore cold-air advection over the Weddell Sea.
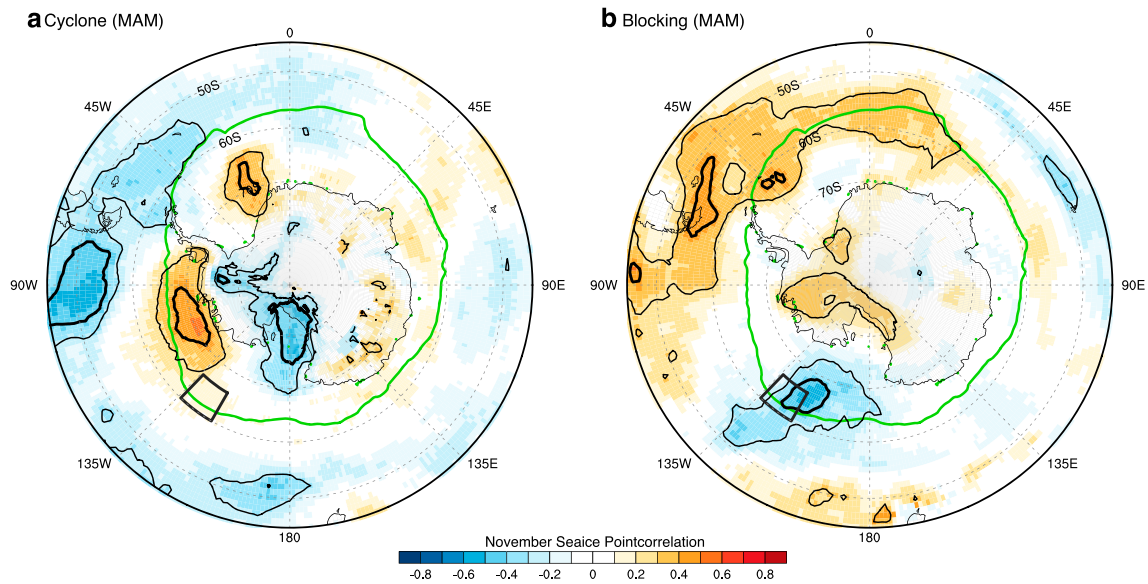
Figure 3. Point-correlation maps between November sea ice fraction, area-averaged over the different target regions (shown as black boxes in every panel), and preceding MAM (a) cyclone and (b) blocking frequencies. The thin black contour indicates statistical significance at the 0.9 level; the bold black contour indicates significance at the 0.99 level. MAM = Autumn (March-April-May).

When the sea ice cyclone frequency correlation patterns for these first two target regions are combined (Figures 2a and 2c), a band of circumpolar positive correlations emerges. At the same time, a circumpolar inverse-correlation band emerges further poleward. This dipole pattern suggests a possible link to the SAM, which is characterized by a north-south migration of synoptic-scale weather systems (Kidson & Sinclair, 1995; Simmonds & Jacka, 1995).

The third target region (labeled 3 in Figure 1a) is located at the transition between the Ross Sea and the Amundsen Sea near 135°W (Figures 2e and 2f). Sea ice extent in this region is closely related to cyclone frequencies and inversely connected with blocking frequencies downstream over the Bellingshausen Sea. The positive connection with cyclone frequencies over the Bellingshausen Sea is therefore opposite that of the inverse connection found previously for the two target regions over the Weddell and Ross Seas. This is broadly consistent with previous studies that identify a dipole in sea ice conditions between the Amundsen-Bellinghausen and Weddell Seas (Lefebvre & Goosse, 2008; Simpkins et al., 2012).

It is relevant to note that a significant lagged correlation exists with cyclone and blocking frequencies during the previous autumn (March-April-May) for this third target region. The connection is strong with autumn cyclone frequency downstream over the Bellingshausen Sea (Figure 3a). An inverse correlation is found with autumn blocking frequency (Figure 3b). Hence, autumn cyclone and blocking frequencies appear to create a propensity for the evolution of sea ice during the following spring. This is not surprising because springtime sea ice extent is the time integral of sea ice intensification rates during the previous seasons; autumn, therefore, sets the initial conditions for the sea ice evolution during the following spring. However, only for this third target region is the lagged correlation significant.

3.2. Autumn (March-April-May)

During the autumn season, significant inverse correlations are found between cyclone frequencies over the Bellingshausen-Amundsen Sea and sea ice extent over the Bellingshausen Sea (Figure 4a). Maximum correlations are shifted upstream relative to the target region. At the same time, a band of significant positive correlations with cyclone frequencies extends at lower latitudes (~50°S) across the Pacific. This pattern suggests that Pacific storm track variability may play a role in determining autumn sea ice conditions. Furthermore, this target region exhibits significant correlations with blocking frequencies upstream (~60°S, 130°W). Such a pronounced block west of the Antarctic Peninsula is a characteristic synoptic flow situation for the Pacific South America Pattern (Kidson, 1988; Mo & Higgins, 1998). The zonal wave number 3 pattern is also
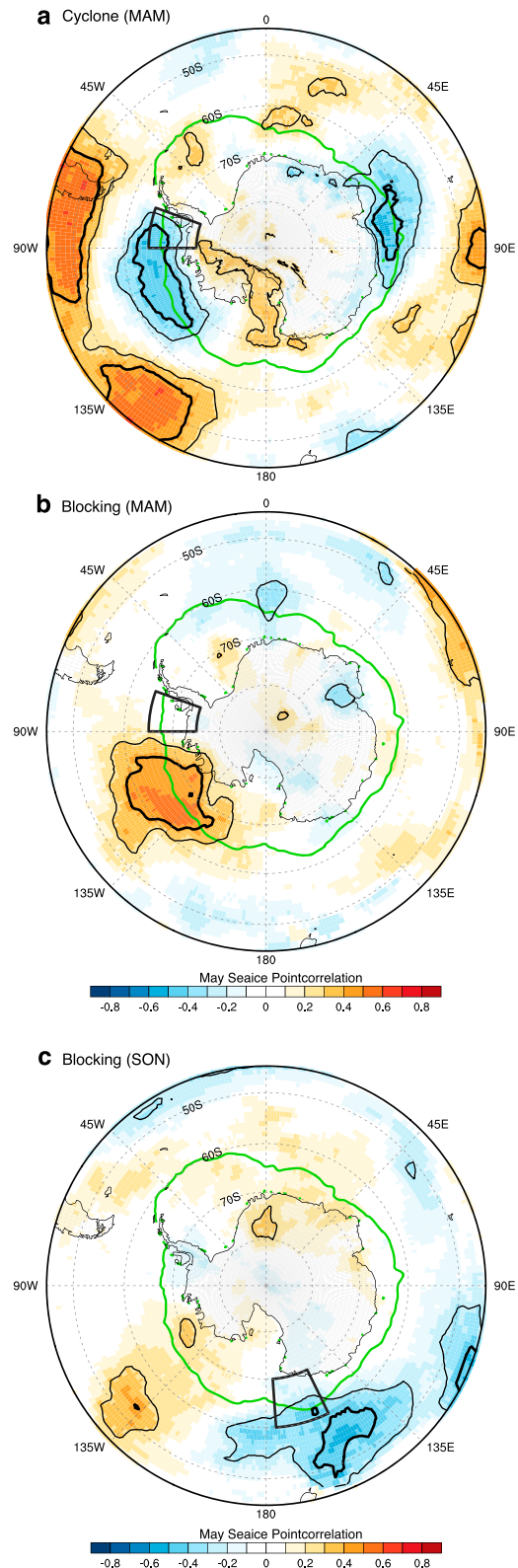
Figure 4. Point-correlation maps between May sea ice fraction, area-averaged over the different target regions (shown as black boxes in every panel), and MAM (a) cyclone frequencies, (b) blocking frequencies, and (c) preceding SON blocking frequency. The thin black contour indicates statistical significance at the 0.9 level; the bold black contour indicates significance at the 0.99 level. MAM = Autumn (March-April-May); SON = Spring (September-October-November).
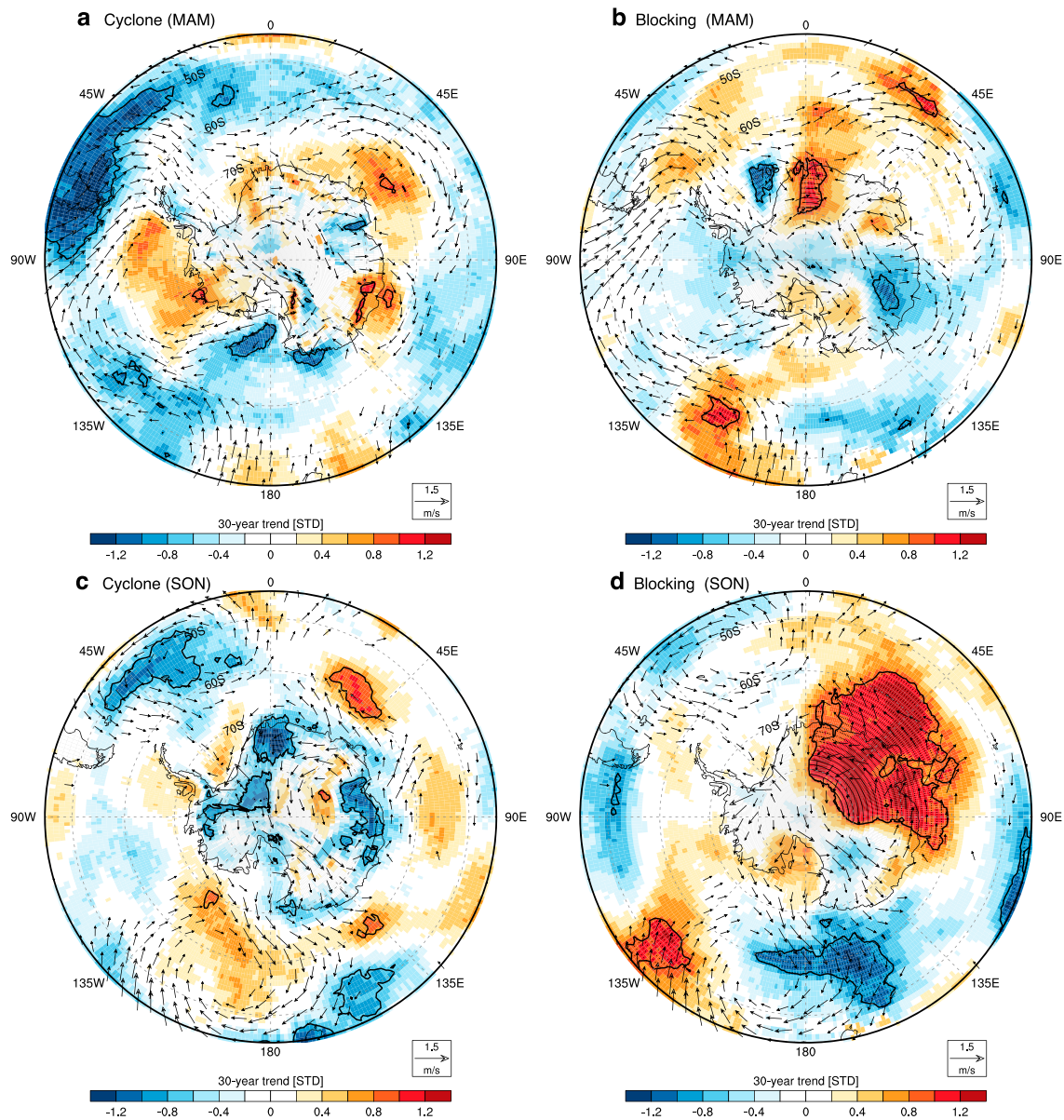
Figure 5. Standardized trends in cyclone (left column) and blocking (right column) frequencies during MAM (a,b) MAM and (c,d) SON and corresponding 10-m wind trends. The thin black contour indicate regions that pass a field significance test (FDR test; see section 2). MAM = Autumn (March-April-May); SON = Spring (September-October-November); FDR = false discovery rate.

known to be associated with enhanced blocking activity (Irving & Simmonds, 2015; Trenberth & Mo, 1985). Consequently, the identified blocking pattern could be used to establish a link to different hemispheric-wide climate modes.

For the second target region west of the Ross Sea (labeled 1 in Figure 1b) no linkage between autumn sea ice and autumn cyclone or blocking frequencies is found but a significant inverse correlation is found with blocking frequencies during the preceding spring. Notably, there is no comparable correlation with cyclone frequencies from the preceding spring. The fact that autumn sea ice conditions are well correlated with the sea ice conditions during the following autumn, and vice versa, is already highlighted by Stammerjohn et al. (2012). Consequently, because springtime blocking exhibits a significant inverse correlation with spring and autumn sea ice extent (cf. Figures 2b and 4c), springtime blocking seems to be able to dictate spring and autumn sea ice conditions in this sector upstream of 180°.

4. Trends in Weather Systems During Autumn and Spring

The previous section helped to connect sea ice extent with cyclone and blocking frequencies in regions that are exposed to long-term sea ice trends. The question arising from this is whether trends exist in the frequencies of both types of weather systems and if these trends are in agreement with the previously discussed linkages with sea ice extent.

4.1. Spring (September-October-November)

In the first target region off the Ross Sea (label 1 in Figure 1a), sea ice extent has increased since 1979 (Figure 1a). In this target region, sea ice extent is strongly connected to seasonal cyclone frequencies and inversely connected to blocking frequencies. The trends in both types of weather systems agree in sign with the increase in sea ice extent (Figures 5c and 5d), but only the downward trend in blocking frequency upstream of 180° is field significant and therefore potential a key driver behind the observed increase in sea ice extent.

The second target region, located along the Weddell Sea's ice edge, experiences a downward trend in sea ice extent (label 2 in Figure 1a). The correlation of sea ice extent with seasonal cyclone frequencies is significant and positive downstream of the target region (Figure 2c). A significant downward trend in cyclone frequency exists in this area (Figure 5c) and is therefore in agreement with the trend in sea ice extent. This suggests that decreasing cyclone frequencies play a relevant role as drivers behind the reduction in sea ice extent along the Weddell Sea's ice edge. Furthermore, because cyclone activity in this area is known to be strongly linked to the Pacific-South America mode, the decreasing cyclone frequencies provide a potential link between the Pacific-South America and the sea ice edge trend in the Weddell Sea.

The third target region near 135°W (label 3 in Figure 1a), where sea ice extent increases, is significantly connected to spring and autumn cyclone frequencies downstream over the Bellingshausen-Amundsen Sea (Figures 2e and 3a). During spring, cyclone frequencies are not affected by any trend (Figure 5c). However, there is a nonsignificant upward trend in cyclone frequencies in this sector during autumn (Figure 5a), which may therefore contribute to the increase in sea ice extent in this region. (Note that it is significant over a very limited region near the coast).

4.2. Autumn (March-April-May)

Sea ice extent has increased over the first target region west of the Ross Sea (label 1 in Figure 1b). From Figure 4c, we see that a significant inverse correlation exists between sea ice extent and blocking frequencies during the preceding spring. Indeed, a significant decrease in autumn blocking frequencies is identified over this critical region (Figure 5d). Hence, it appears plausible that the reduction in spring blocking frequencies acts as a sea ice trend driver. This decrease in autumn blocking (Figure 5d) and the concomitant increase in autumn cyclone frequency (Figure 5c) are in agreement with long-term trends identified in sea level pressure (cf. Figure 8 in Simmonds, 2015)

The second target region, located in the Bellingshausen Sea (label 2 in Figure 1b), exhibits a downward trend in sea ice extension. Sea ice extent in this region is significantly correlated with upstream blocking frequency and also exhibits a strong inverse correlation with cyclone frequency (Figures 4a and 4b). The corresponding cyclone and blocking trend patterns (Figures 5a and 5b) suggest an increase in cyclone frequency and a decrease in blocking frequency. The increase in cyclone frequency, though nonsignificant, is therefore in agreement with the reduction in sea ice extent. Furthermore, the increase in cyclone frequency is consistent with the significant downward trend in sea level pressure found by Simmonds (2015).

5. Concluding Remarks

While many of the underlying processes that affect sea ice extent are known (e.g., 10-m wind as a mechanical and thermodynamic agent; Holland & Kwok, 2012; Massom et al., 2008; Mayewski et al., 2009; Stammerjohn et al., 2003; Turner et al., 2016), it remains challenging to connect hemispheric-wide climate trends in sea ice extent (Kwok et al., 2016; Pezza et al., 2012; Simmonds & Jacka, 1995; Simpkins et al., 2012; Stammerjohn et al., 2008). To bridge the large spatial and temporal scales between these two phenomena, analyses of weather systems and their dynamics provide the necessary intermediate step (Pezza et al., 2012). To date, most researches have focused on links between extratropical cyclones with the Amundsen Sea Low (Fogt et al., 2012; Raphael et al., 2016; Turner et al., 2016) or have focused on the (local) role of blocks on Antarctic sea ice conditions (Massom et al., 2006, 2008). The trends in cyclone and blocking frequencies reported here

provide a means for understanding hemispheric-wide climate changes and the regional inhomogeneity of the Antarctic sea ice trends. In general, this study shows that the connection between weather systems and sea ice extent is strongest near the sea ice edge and correlations peak up or downstream of the sea ice target region. The detailed findings for spring (September-October-November) can be summarized as follows:

1. East of the Ross Sea, sea ice extent has increased (Figure 1a) and a significant (inverse) correlation with (blocking) cyclone frequencies exists. Maximum correlations with (blocking) cyclone frequencies are shifted slightly (upstream) downstream of the target region (Figures 2a and 2b). Blocking frequency has significantly decreased upstream and is therefore in agreement with the sea ice trend.
2. Along the Weddell Sea's ice edge, sea ice extent has decreased (Figure 1a) and is significantly correlated with downstream cyclone and upstream blocking frequencies (Figures 2c and 2d). Indeed, a significant decrease in cyclone frequency is found downstream of the southern tip of South America (Figure 5c). This reduction in cyclone frequencies could be a plausible explanation for the more northerly (onshore) trend in the 10-m winds seen in this region.
3. Sea ice extent along the transition zone from the Ross into the Amundsen Sea is strongly connected to cyclone frequencies downstream over the Bellingshausen Sea (Figures 2e and 2f). Additionally, an inverse connection exists with blocking frequency. In contrast to the first two target regions, a significant (inverse) connection also exists with cyclone (blocking) frequencies during the preceding autumn (Figures 3a and 3b). The Bellingshausen Sea does not experience a change in springtime cyclone frequencies. Therefore, it is likely that the increase in springtime sea ice extent is partly related to an increase in autumn cyclone frequencies over the Bellingshausen Sea.

The correlation between sea ice and cyclone frequency for the first two target regions display a zonal wave number 3 pattern (Figures 2a and 2c), while those with blocking frequencies display a zonal wave number 2 pattern (Figure 2d).

For the autumn season (March-April-May), the following findings are relevant:

1. Sea ice extent has decreased over the Bellingshausen Sea (Figure 1b). Sea ice extent in this region displays a significant (inverse) connection with upstream (cyclone) blocking frequencies (Figures 4a and 4b). The negative sea ice trend is therefore in agreement with an increase in cyclone frequency in this region (Figure 5a). The increase in cyclone frequency, though not significant (according to the used method), it is in agreement with a significant downward trend in sea level pressure (cf. Figure 7b in Simmonds, 2015)
2. Sea ice extent has increased east of the Ross Sea (Figure 1b) and is significantly anticorrelated with blocking frequencies from the preceding spring. Indeed, springtime blocking frequencies have significantly decreased over the relevant region (Figure 5d) and therefore appear to be the number one candidate for explaining the observed autumn sea ice trends. Note, that this is the same trend in blocking frequency that is related to a positive springtime trend in sea ice (cf. Figures 2b, 4c, and 5d).

This study demonstrates that in almost all regions that exhibit strong trends in sea ice extent also exhibit concomitant trends in the frequency of cyclones or blocks, sometimes across seasons. Often, the trends are significant but, as noted in section 2, statistical significance depends on the used cyclone tracking scheme, while the trend sign is more robust across cyclone tracking schemes (Grieger et al., 2018). A natural extension of this study would be to connect the trends in both types of weather systems to measures of Southern Hemisphere climate variability such as the SAM, the Pacific-South America Pattern, or the zonal wave number 3 pattern.

References

Comiso, J. C., Gersten, R. A., Stock, L. V., Turner, J., Perez, G. J., & Cho, K. (2017). Positive trend in the Antarctic sea ice cover and associated changes in surface temperature. *Journal of Climate*, *30*, 2251–2267. https://doi.org/10.1175/JCLI-D-16-0408.1

Croci-Maspoli, M., Schwierz, C., & Davies, H. C. (2007). Atmospheric blocking: Space-time links to the NAO and PNA. *Climate Dynamics*, *29*, 713–725. https://doi.org/10.1007/s00382-007-0259-4

Fogt, R. L., Wovrosh, A. J., Langen, R. A., & Simmonds, I. (2012). The characteristic variability and connection to the underlying synoptic activity of the Amundsen-Bellingshausen seas low. *Journal of Geophysical Research*, *117*, D07111. https://doi.org/10.1029/2011JD017337

Goosse, H., & Zunz, V. (2014). Decadal trends in the Antarctic sea ice extent ultimately controlled by ice–ocean feedback. *The Cryosphere*, *453–470*. https://doi.org/10.5194/tc-8-453-2014

Grieger, J., Leckerbusch, G. C., Raible, C. C., Rudeva, I., & Simmonds, I. (2018). Subantarctic cyclones identified by 14 tracking methods, and their role for moisture transports into the continent. *Tellus A: Dynamic Meteorology and Oceanography*, *70*, 1454808. https://doi.org/10.1080/16000870.2018.1454808

Hobbs, W. R., Massom, R., Stammerjohn, S., Reid, P., Williams, G., & Meier, W. (2016). A review of recent changes in Southern Ocean sea ice, their drivers and forcings. *Global and Planetary Change*, *143*, 228–250. https://doi.org/10.1016/j.gloplacha.2016.06.008

Holland, P. R. (2014). The seasonality of Antarctic sea ice trends. *Geophysical Research Letters*, *41*, 4230–4237. https://doi.org/10.1002/2014GL060172

Holland, P. R., & Kwok, R. (2012). Wind-driven trends in Antarctic sea ice drift. *Nature Geoscience*, *5*, 872–875. https://doi.org/10.1038/ngeo1627

Holland, M. M., Landrum, L., Raphael, M., & Stammerjohn, S. (2017). Springtime winds drive Ross sea ice variability and change in the following autumn. *Nature Communications*, *8*, 731. https://doi.org/10.1038/s41467-017-00820-0

Irving, D., & Simmonds, I. (2015). A novel approach to diagnosing Southern Hemisphere planetary wave activity and its influence on regional climate variability. *Journal of Climate*, *28*, 9041–9057. https://doi.org/10.1175/JCLI-D-15-0287.1

Kidson, J. W. (1988). Indices of the Southern Hemisphere zonal wind. *Journal of Climate*, *1*(2), 183–194. https://doi.org/10.1175/1520-0442(1988)001<0183:iotshz>2.0.co;2

Kidson, J. W., & Sinclair, M. R. (1995). The influence of persistent anomalies on Southern Hemisphere storm tracks. *Journal of Climate*, *8*(8), 1938–1950.

Kwok, R., Comiso, J. C., Lee, T., & Holland, P. R. (2016). Linked trends in the South Pacific sea ice edge and southern oscillation index. *Geophysical Research Letters*, *43*, 10,295–10,302. https://doi.org/10.1002/2016GL070655

Lefebvre, W., & Goosse, H. (2005). Influence of the Southern Annular Mode on the sea ice-ocean system: The role of the thermal and mechanical forcing. *Ocean Science*, *1*, 145–157. https://doi.org/10.5194/os-1-145-2005

Lefebvre, W., & Goosse, H. (2008). An analysis of the atmospheric processes driving the large-scale winter sea ice variability in the Southern Ocean. *Journal of Geophysical Research*, *113*, C02004. https://doi.org/10.1029/2006JC004032

Lefebvre, W., Goosse, H., Timmermann, R., & Fichefet, T. (2004). Influence of the Southern Annular Mode on the sea ice–ocean system. *Journal of Geophysical Research*, *109*, C09005. https://doi.org/10.1029/2004JC002403

Liu, J., & Curry, J. A. (2010). Accelerated warming of the Southern Ocean and its impacts on the hydrological cycle and sea ice. *Proceedings of the National Academy of Sciences of the United States of America*, *107*, 14,987–14,992. https://doi.org/10.1073/pnas.1003336107

Marshall, G. J. (2003). Trends in the Southern Annular Mode from observations and reanalyses. *Journal of Climate*, *16*(24), 4134–4143. https://doi.org/10.1175/1520-0442(2003)016<4134:TITSAM>2.0.CO;2

Massom, R. A., Stammerjohn, S. E., Lefebvre, W., Harangozo, S. A., Adams, N., Scambos, T. A., et al. (2008). West Antarctic Peninsula sea ice in 2005: Extreme ice compaction and ice edge retreat due to strong anomaly with respect to climate. *Journal of Geophysical Research*, *113*, C02S20. https://10.1029/2007JC004239

Massom, R. A., Stammerjohn, S. E., Smith, R. C., Pook, M. J., Iannuzzi, R. A., Adams, N., et al. (2006). Extreme anomalous atmospheric circulation in the West Antarctic Peninsula region in austral spring and summer 2001/02, and its profound impact on sea ice and biota. *Journal of Climate*, *19*, 3544–3571. https://doi.org/10.1175/jcli3805.1

Mayewski, P. A., Meredith, M. P., Summerhayes, C. P., Turner, J., Worby, A., Barrett, P. J., et al. (2009). State of the Antarctic and Southern Ocean climate system. *Reviews of Geophysics*, *47*, RG1003. https://doi.org/10.1029/2007RG000231

Meier, W., Fetterer, F., Savoie, M., Mallory, S., Duerr, R., & Stroeve, J. (2017). *NOAA/NSIDC climate data record of passive microwave sea ice concentration, version 3*. Boulder, Colorado USA. NSIDC: National Snow and Ice Data Center. https://doi.org/10.7265/N59P2ZTG

Mo, K. C., & Higgins, R. W. (1998). The Pacific–South American Modes and tropical convection during the Southern Hemisphere winter. *Monthly Weather Review*, *126*(6), 1581–1596. https://doi.org/10.1175/1520-0493(1998)126<1581:tpsama>2.0.co;2

Neu, U., Akperov, M. G., Bellenbaum, N., Benestad, R., Blender, R., Caballero, R., et al. (2013). IMILAST: A community effort to intercompare extratropical cyclone detection and tracking algorithms. *Bulletin of the American Meteorological Society*, *94*, 529–547. https://doi.org/10.1175/BAMS-D-11-00154.1

Parkinson, C. L., & Cavalieri, D. J. (2012). Antarctic sea ice variability and trends, 1979–2010. *The Cryosphere*, *6*, 871–880. https://doi.org/10.5194/tc-6-871-2012

Peng, G., Meier, W. N., Scott, D. J., & Savoie, M. H. (2013). A long-term and reproducible passive microwave sea ice concentration data record for climate studies and monitoring. *Earth System Science Data*, *5*, 311–318. https://doi.org/10.5194/essd-5-311-2013

Pezza, A. B., Rashid, H. A., & Simmonds, I. (2012). Climate links and recent extremes in Antarctic sea ice, high-latitude cyclones, Southern Annular Mode and ENSO. *Climate Dynamics*, *38*, 57–73. https://doi.org/10.1007/s00382-011-1044-y

Pope, J. O., Holland, P. R., Orr, A., Marshall, G. J., & Phillips, T. (2016). The impacts of El Niño on the observed sea ice budget of West Antarctica. *Geophysical Research Letters*, *44*, 6200–6208. https://doi.org/10.1002/2017GL073414

Raphael, M. N., Marshall, G. J., Turner, J., Fogt, R. L., Schneider, D., Dixon, D. A., et al. (2016). The Amundsen sea low: Variability, change, and impact on Antarctic climate. *Bulletin of the American Meteorological Society*, *97*, 111–121. https://doi.org/10.1175/bams-d-14-00018.1

Schwierz, C., Croci-Maspoli, M., & Davies, H. C. (2006). Perspicacious indicators of atmospheric blocking. *Geophysical Research Letters*, *31*, L06125. https://doi.org/10.1029/2003GL019341

Simmonds, I. (2015). Comparing and contrasting the behaviour of Arctic and Antarctic sea ice over the 35 year period 1979–2013. *Annals of Glaciology*, *56*, 18–28. https://doi.org/10.3189/2015AoG69A909

Simmonds, I., & Jacka, T. H. (1995). Relationships between the interannual variability of Antarctic sea ice and the Southern Oscillation. *Journal of Climate*, *8*(3), 637–647. https://doi.org/10.1175/1520-0442(1995)008<0637:rbtivo>2.0.co;2

Simpkins, G. R., Ciasto, L. M., Thompson, D. W. J., & England, M. H. (2012). Seasonal relationships between large-scale climate variability and Antarctic sea ice concentration. *Journal of Climate*, *25*, 5451–5469. https://doi.org/10.1175/jcli-d-11-00367.1

Sprenger, M., Fragkoulidis, G., Binder, H., Croci-Maspoli, M., Graf, P., Grams, C. M., et al. (2017). Global climatologies of Eulerian and Lagrangian flow features based on ERA-Interim. *Bulletin of the American Meteorological Society*, *98*, 1739–1748. https://doi.org/10.1175/BAMS-D-15-00299.1

Stammerjohn, S. E., Drinkwater, M. R., Smith, R. C., & Liu, X. (2003). Ice-atmosphere interactions during sea ice advance and retreat in the Western Antarctic Peninsula region. *Journal of Geophysical Research*, *108*, 3329. https://doi.org/10.1029/2002JC001543

Stammerjohn, S. E., Martinson, D. G., Smith, R. C., Yuan, X., & Rind, D. (2008). Trends in Antarctic annual sea ice retreat and advance and their relation to El Niño–Southern Oscillation and Southern Annular Mode variability. *Journal of Geophysical Research*, *113*, C03S90. https://doi.org/10.1029/2007JC004269

Stammerjohn, S., Massom, R., Rind, D., & Martinson, D. (2012). Regions of rapid sea ice change: An inter-hemispheric seasonal comparison. *Geophysical Research Letters*, *39*, L06501. https://doi.org/10.1029/2012GL050874

Stammerjohn, S. E., & Smith, R. C. (1997). Opposing Southern Ocean climate patterns as revealed by trends in regional sea ice coverage. *Climatic Change*, *37*(4), 617–639. https://doi.org/10.1023/A:1005331731034

Thompson, D. W. J., & Solomon, S. (2002). Interpretation of recent Southern Hemisphere climate change. *Science*, *296*, 895–899. https://doi.org/10.1126/science.1069270

Trenberth, K. F., & Mo, K. C. (1985). Blocking in the Southern Hemisphere. *Monthly Weather Review*, *113*(1), 3–21. https://doi.org/10.1175/1520-0493(1985)113<0003:bitsh>2.0.co;2

Turner, J., Bracegirdle, T. J., Phillips, T., Marshall, G. J., & Hosking, J. S. (2013). An initial assessment of Antarctic sea ice extent in the CMIP5 models. *Journal of Climate*, *26*, 1473–1484. http://doi.org/10.1175/JCLI-D-12-00068.1

Turner, J., Hosking, J. S., Marshall, G. J., Phillips, T., & Bracegirdle, T. J. (2016). Antarctic sea ice increase consistent with intrinsic variability of the Amundsen Sea Low. *Climate Dynamics*, *46*, 2391–2402. https://doi.org/10.1007/s00382-015-2708-9

Wernli, H., & Schwierz, C. (2006). Surface cyclones in the ERA-40 dataset (1958–2001). Part I: Novel identification method and global climatology. *Journal of the Atmospheric Sciences*, *63*, 2486–2507. https://doi.org/10.1175/JAS3766.1

Wilks, D. S. (2016). "The stippling shows statistically significant grid points": How research results are routinely overstated and overinterpreted, and what to do about it. *Bulletin of the American Meteorological Society*, *97*, 2263–2273. https://doi.org/10.1175/bams-d-15-00267.1

Zhang, J. (2007). Increasing Antarctic sea ice under warming atmospheric and oceanic conditions. *Journal of Climate*, *20*, 2515–2529. https://doi.org/10.1175/JCLI4136.1